

Astronomy & Astrophysics manuscript no.  
(will be inserted by hand later)

# Detection of a multi-phase ISM at $z = 0.2212$ .

Nissim Kanekar<sup>1</sup>\*, Tapasi Ghosh<sup>2</sup>\*\*, Jayaram N Chengalur<sup>1</sup>\*\*\*

<sup>1</sup> National Centre for Radio Astrophysics, Post Bag 3, Ganeshkhind, Pune 411 007

<sup>2</sup> NAIC, Arecibo Observatory, HC 3 Box 53995, Arecibo, PR00612, USA

Received mmddyy/ accepted mmddyy

**Abstract.** We present sensitive Giant Metrewave Radio Telescope (GMRT) and high-resolution Arecibo HI 21-cm observations of the damped Lyman- $\alpha$  absorber (DLA) at  $z = 0.2212$  towards OI 363 ( $B2\ 0738+313$ ). The GMRT and Arecibo spectra are in excellent agreement and yield a spin temperature  $T_s = 890 \pm 160$  K, consistent with earlier lower sensitivity observations of the system. This value of  $T_s$  is far higher than spin temperatures measured for the Milky Way and local spirals but is similar to  $T_s$  values obtained in the majority of damped absorbers ( $T_s \gtrsim 1000$  K).

The high velocity resolution of the Arecibo spectra enables us to obtain estimates of physical conditions in the absorbing clouds by fitting multiple Gaussians to the absorption profile. The spectra are well fit by a three-component model with two narrow and one wide components, with temperatures  $T_{k_1} = 308 \pm 24$  K,  $T_{k_2} = 180 \pm 30$  K and  $T_{k_3} = 7600 \pm 1250$  K, respectively. The last of these is in excellent agreement with the expected temperatures for the WNM (5000 – 8000 K). Further, the mere fact that components are seen with lower temperatures than the estimated  $T_s$  implies that the absorber must have a multi-phase medium.

We use the measured 21-cm optical depth and the above estimates of the kinetic temperature to obtain the HI column density in the various components. The total column density in the narrow components is found to be  $N_{\text{HI}}(\text{CNM}) \leq 1.9 \pm 0.25 \times 10^{20} \text{ cm}^{-2}$ , while that in the wide component is  $N_{\text{HI}}(\text{WNM}) \geq 1.26 \pm 0.49 \times 10^{21} \text{ cm}^{-2}$ . Thus, the WNM contains at least 75 % of the total HI in the  $z = 0.2212$  DLA, unlike our Galaxy, in which the CNM and WNM have equitable contributions. As conjectured earlier (Chengalur & Kanekar 2000), this accounts for the difference in the spin temperatures of the  $z = 0.2212$  system and local spirals, suggesting that the DLA is probably a dwarf or LSB type galaxy; this is also in agreement with optical studies (Turnshek et al. 2001). Finally, the total column density in the DLA is found to be  $N_{\text{HI}} \sim 1.45 \pm 0.49 \times 10^{21} \text{ cm}^{-2}$ , which agrees within the errors with the value of  $N_{\text{HI}} = 7.9 \pm 1.4 \times 10^{20} \text{ cm}^{-2}$ , obtained from the Lyman- $\alpha$  profile (Rao & Turnshek 1998). This reinforces our identification of the wide and narrow components as the WNM and CNM respectively.

**Key words.** galaxies: evolution: – galaxies: formation: – galaxies: ISM – cosmology: observations – radio lines: galaxies

## 1. Introduction

Extragalactic gas clouds which lie along the line of sight to a distant quasar give rise to absorption lines in the quasar spectrum. For clouds with neutral hydrogen column density  $N_{\text{HI}} \gtrsim 10^{20} \text{ cm}^{-2}$ , the width of the absorption line corresponding to the Lyman- $\alpha$  transition is very large because the optical depth is substantial even in the Lorenzian wings of the line profile. Essentially, at these column densities, the shape of the absorption profile is determined not by the Doppler motions of the atoms in the cloud, but by the natural profile of the line. These high column density systems (called damped

Lyman- $\alpha$  absorbers, or DLAs) are rare – the probability of finding a DLA in a random search towards a high redshift quasar is  $\sim 0.25$  per unit redshift interval (Storrie-Lombardi & Wolfe 2000). Nonetheless, DLAs contain the bulk of the observed neutral gas at high redshift ( $z \sim 3$ ) and are hence logical candidates for the precursors of today's galaxies.

Since quasars are essentially point-like objects in the optical and UV wavebands, their absorption spectra in these bands contain information only on the gas illuminated by the narrow pencil beam of continuum emission from the quasar. It is largely for this reason that the typical transverse size, luminosity and mass of DLAs remain controversial despite almost two decades of systematic study. Damped systems at high redshift have traditionally been assumed to be disk galaxies (e.g. Wolfe 1988). Some support for this hypothesis is provided by high spectral

Send offprint requests to: Nissim Kanekar

\* nissim@ncra.tifr.res.in

\*\* tghosh@naic.edu

\*\*\* chengal@ncra.tifr.res.in

resolution optical studies of the absorption profiles of low ionization metals in the absorbers. These metals have ionization potentials lower than that of HI, as well as unsaturated line profiles; these profiles thus trace the kinematics of the neutral gas in the DLA (Lanzetta & Bowen 1992). Prochaska & Wolfe (1997, 1998; but see Ledoux et al. 1998) used a large sample of DLAs to argue that the metal line profiles were consistent with those arising from rapidly rotating massive disks. However, it was later shown that such profiles could also be generated in a variety of DLA models, ranging from merging sub-galactic blobs (Haehnelt et al. 1998), to randomly moving clouds in a spherical halo (McDonald & Miralda-Escude 1999). At low redshifts, Hubble Space Telescope (HST) and ground-based imaging and spectroscopy can be used to carry out detailed studies of the galaxies responsible for the damped absorption. These observations indicate that DLAs are associated with a wide variety of galaxy types and are not exclusively (or even predominantly) spiral galaxies (Le Brun et al. 1997, Rao & Turnshek 1998, Turnshek et al. 2000). In this paper, we will discuss HI 21-cm observations of the DLA at  $z = 0.2212$  toward the radio-loud quasar OI 363 ( $B2\ 0738 + 313$ ); this absorber has been identified by recent studies as a dwarf, or possibly LSB-type, galaxy, with luminosity  $L \sim 0.1L_*$  (Turnshek et al. 2001, Cohen 2001).

HI 21-cm absorption was first detected in the DLA at  $z = 0.2212$  by Lane et al. (1998), using the Westerbork Synthesis Radio Telescope (WSRT); these observations, however, only marginally resolved the line. A higher sensitivity, higher resolution spectrum using the Giant Metrewave Radio Telescope (GMRT) was presented by Chengalur & Kanekar (1999). This 21-cm profile showed a single, narrow component with  $\text{FWHM} \sim 5.5 \text{ km s}^{-1}$  and was used to estimate the spin temperature of the absorbing gas. This was found to be quite high,  $T_s = 1120 \pm 200 \text{ K}$ . In the Galaxy, gas with a temperature of  $\sim 1000 \text{ K}$  is unstable. In standard models of the galactic interstellar medium (ISM) (Wolfire et al. 1995, Kulkarni & Heiles 1988), neutral hydrogen exists in only two stable phases, a cold phase at  $\sim 80 \text{ K}$  and a warm phase at  $\sim 8000 \text{ K}$ . For a multi-phase medium, however, the measured spin temperature is the column density weighted harmonic mean of the temperatures of the different phases. It was hence proposed that the high values of  $T_s$  estimated for this and other DLAs were due to a substantial fraction of their neutral gas being in the warm phase (Chengalur & Kanekar 2000, Kanekar & Chengalur 2001).

Here, we present high-resolution Arecibo HI 21-cm observations of the  $z = 0.2212$  absorber, supplemented by a deep GMRT 21-cm observation of the system. These observations enable us to directly determine the kinetic temperature of the absorbing gas and thus, to distinguish between the warm and cold phases. We find, as conjectured previously, that the bulk of the gas is indeed in the warm phase, which contains at least three-fourths of the total HI along this line of sight. This is the second DLA

for which it has been observationally established that a high spin temperature is due to a preponderance of gas in the warm neutral medium; Lane et al. (2000) show that this phase contains at least two-thirds of the gas in a DLA at  $z = 0.0912$  (also, coincidentally, towards OI 363).

The rest of the paper is organised as follows: the GMRT and Arecibo observations and data analysis are described in Sect. 2. Sect. 3 presents the absorption spectra; the spin temperature of the absorber and the temperatures of the different absorbing components are also estimated here. Finally, Sect. 4 discusses our results both in the context of observations of the  $z = 0.2212$  DLA at other wavelengths, and with respect to their general implications for the nature of systems which give rise to damped Lyman- $\alpha$  absorption.

## 2. Observations and data analysis

### 2.1. Arecibo observations and data analysis.

The  $z = 0.2212$  absorber towards OI 363 was observed on a number of occasions in February, April and August 2000, using the 305-m Arecibo radio telescope. All observations were done in total power mode, with the “L-wide” receiver, using 9-level sampling for the auto-correlation spectrometer. Two orthogonal circular polarization channels were observed simultaneously. The first two sessions (in February and April 2000) used bandwidths of 3.125 and 6.25 MHz, centred at a heliocentric redshift of  $z = 0.2212$ , and divided into 2048 channels. This yielded velocity resolutions of  $0.3935$  and  $0.79 \text{ km s}^{-1}$  respectively.

OI 363 has substantial continuum flux density ( $\sim 2 \text{ Jy}$ ) at L band and the bandpass is hence dominated by systematics due to standing wave patterns. To improve the bandpass calibration, the observations were carried out in a “double switched” mode. OI 363 was observed first, followed by an observation of blank sky. Next, a similar position-switched observation was made for a nearby source, OI 371 ( $B\ 0742+318$ , flux density  $\sim 1.4 \text{ Jy}$ ). OI 363 and OI 371 have very similar declinations and continuum flux densities; the observations were so timed that the alt-az track of the feed was almost the same for all phases of the observing cycle. Each of these phases was  $\sim 4$  minutes long (with 5-second data records) and this cycle was repeated on each observing day for as long as the sources were visible from Arecibo. All observations were carried out at night, to minimise solar effects. The total on-source time for OI 363 was about 9 hours.

A second set of observations was carried out in August 2000, with the aim of better resolving the narrow absorption components seen in the initial Arecibo observations. Far smaller bandwidths of 0.781 and 0.195 MHz were hence used, again divided into 2048 channels, and with two polarizations at each setting. This gave velocity resolutions of  $\sim 0.099$  and  $\sim 0.025 \text{ km s}^{-1}$  respectively. These observations were carried out in the standard on-off position switching mode (i.e. a single blank sky spectrum was used to calibrate the bandpass), since the wider

of the two bandwidths (0.781 MHz) was narrower in frequency than one cycle of the standing wave ripple (which is  $\sim 1$  MHz at Arecibo). Each on-off cycle was of five minutes duration, sub-divided into 1-second records. The total on-source time was  $\sim 35$  minutes.

The data for both sets of observations were reduced using the Arecibo software package ANALYZ. For the February and April observations, each four-minute spectrum was initially inspected for radio frequency interference (RFI). If interference was seen, the individual 5-sec records of the four-minute run were passed through a standard RFI excision program, and all records with strong ( $> 10\sigma$ ) features were removed. Each four-minute spectrum was also inspected for the presence of standing waves. It was found that the fluctuations on each such position-switched spectrum were indeed dominated by standing waves across the bandpass. However, when an OI 363 spectrum was divided by the corresponding spectrum of OI 371 using the formula,

$$\text{Spectrum} = \left[ \frac{\text{On} - \text{Off}}{\text{Off}} \right]_{\text{OI 363}} \bigg/ \left[ \frac{\text{On} - \text{Off}}{\text{Off}} \right]_{\text{OI 371}} \quad (1)$$

the resultant spectrum contained essentially Gaussian noise. This ratio of the two spectra was also bandpass corrected and had no remaining effects from the azimuth/zenith-angle dependence of gain. It was then multiplied by the flux density of OI 371 (taken to be 1.4 Jy at 1160 MHz) to convert the spectrum into Jy.

The basic data editing for the August spectrum was carried out in a similar manner. Here, however, the individual five-minute spectra were obtained by the formula

$$\text{Spectrum} = \left[ \frac{\text{On} - \text{Off}}{\text{Off}} \right]_{\text{OI 363}} \quad (2)$$

The spectra were then corrected for the System Equivalent Flux Density (SEFD) v/s Zenith angle dependence, to obtain the final spectra in Jy.

For all data sets, the above procedure was carried out separately for the two polarizations. Individual four- and five-minute spectra were averaged together (using the appropriate weights) to produce the final spectrum for each bandwidth. A linear baseline was then fitted to these spectra (excluding the location of the line) and subtracted. Finally, the spectra were divided by the mean continuum flux density to convert them into optical depth (since the line is optically thin, a simple division by the continuum level suffices to convert from flux density into optical depth).

## 2.2. GMRT observations and data analysis.

GMRT observations of the  $z = 0.2212$  absorber were carried out on 19 October, 2000. The standard 30-station FX correlator, which gives a fixed number of 128 channels over a bandwidth which can be varied between 64 kHz and 16 MHz, was used as the backend. A bandwidth of 1 MHz was

used for the observations, yielding a spectral resolution of  $\sim 2.0$  km s $^{-1}$ . 3C147 and 3C286 were used to calibrate the absolute flux density scale and system bandpass; no phase calibrator was used since OI 363 is itself unresolved by the GMRT. The total on-source time was around four and a half hours, with sixteen antennas present.

The data were analysed in AIPS using standard procedures. The analysis was fairly straightforward since there is negligible extended emission in the OI 363 field. Continuum emission was subtracted by fitting a linear baseline to the U-V visibilities, using the AIPS task UVLIN. The continuum subtracted data were then mapped in all frequency channels and a spectrum extracted at the quasar location from the resulting three-dimensional data cube. Spectra were also extracted at other locations in the cube to ensure that the data were not corrupted by interference. A spectrum was also obtained by simply vector averaging the U-V visibilities together, using the AIPS task POSSM. Since the two methods are essentially equivalent for the present case of a point source at the telescope phase centre, we use the POSSM spectrum in the discussion below. The RMS noise on this spectrum is  $\sim 2.8$  mJy, while the flux density of OI 363 was measured to be 2.25 Jy. Our experience with the GMRT indicates that the flux density calibration is reliable to  $\sim 15\%$ , in this observing mode.

## 3. The temperature of the absorbing gas.

The spectra are shown in Fig. 1 and Fig. 2. Fig. 1[A] presents the final Arecibo 3.125-MHz ( $\sim 0.395$  km s $^{-1}$  resolution) spectrum in open squares. This has been smoothed to a resolution of  $\sim 2$  km s $^{-1}$  to compare it to the GMRT spectrum, shown here as a thin solid line. The agreement between the two is excellent. The central narrow absorption component can be seen to be slightly asymmetric in both spectra. Further, in addition to the deep narrow component, the 21-cm spectrum also has a shallow broad component, seen in both the Arecibo and the GMRT spectra. This component can be more clearly seen in the zoomed-in plot of Fig. 1[B], where the two spectra have again been superposed; again, the solid line is the GMRT spectrum, while the open squares are the points on the Arecibo 3.125-MHz spectrum. Fig. 1[C] shows the Arecibo 3.125-MHz spectrum at the original resolution of  $\sim 0.4$  km s $^{-1}$  (open squares); the thin solid line is the multi-Gaussian fit to the spectrum which will be discussed later. This spectrum has an RMS noise of  $\sim 0.001$  in optical depth per  $\sim 0.4$  km s $^{-1}$  channel (i.e.  $\sim 2$  mJy). The deepest absorption occurs at a heliocentric frequency of 1163.075 MHz, i.e. at a heliocentric redshift of  $z = 0.221250 \pm 0.000001$ .

### 3.1. The spin temperature

For optically thin absorption by a homogenous HI cloud, the 21-cm optical depth  $\tau_{21}$  is related to the column density  $N_{\text{HI}}$  and spin temperature  $T_s$  by

$$N_{\text{HI}} = \frac{1.8 \times 10^{18} T_s}{f} \int \tau_{21} dV \quad (3)$$

where  $f$  is the covering factor of the absorbing gas. OI 363 is a highly compact radio source (Lane et al. 2000, Stanghellini et al. 1997) and, as discussed in Chengalur & Kanekar (1999) and Lane et al. (2000), the covering factor of the absorber is likely to be close to unity. As mentioned in Sect. 1, the earlier, lower sensitivity GMRT observations of Chengalur & Kanekar (1999) yielded a high spin temperature  $T_s = 1120 \pm 200$  K for the absorber. The deeper Arecibo observations can be used to obtain a more precise estimate of the spin temperature of the system. The 3.125-MHz Arecibo spectrum was used for this purpose as this, of all the Arecibo spectra, provides the optimum balance between resolution and signal-to-noise ratio. The integrated optical depth of the spectrum in Fig. 1[C] gives an HI column density of  $N_{\text{HI}} = 0.889 \pm 0.007 \times 10^{18} T_s \text{ cm}^{-2}$  for the absorbing gas. The column density obtained from the HST Lyman- $\alpha$  profile is  $N_{\text{HI}} = 7.9 \pm 1.4 \times 10^{20} \text{ cm}^{-2}$  (Rao & Turnshek 1998). Comparing the two yields a spin temperature  $T_s = 890 \pm 160$  K, which agrees within the errors with the values obtained earlier by Lane et al. (1998) and Chengalur & Kanekar (1999).

In the Galaxy, the neutral ISM has no stable phase with a temperature of  $\sim 1000$  K (**although recent Arecibo observations indicate that a significant fraction of neutral gas may be in the unstable phase with  $500 \text{ K} < T_k < 5000 \text{ K}$ ; Heiles & Troland 2000, Heiles 2001**). Instead, there exists a cold phase (the Cold Neutral Medium – CNM) with a temperature of  $\sim 80$  K and a warm phase (the Warm Neutral Medium – WNM) with a temperature of  $\sim 8000$  K. For each individual phase, the spin temperature is essentially the same as the kinetic temperature of the gas. However, the *measured* spin temperature for a multi-phase absorber is the column density weighted harmonic mean of the temperatures of the different phases (provided that the optical depth of the gas in each phase is small; see e.g. Kulkarni & Heiles 1988). The high spin temperature of the  $z = 0.2212$  DLA suggests that the bulk of its neutral gas is in the warm phase, if it has a multi-phase ISM similar to that of the Galaxy.

### 3.2. Temperatures of the individual phases: detection of the WNM

The high resolution and sensitivity of the Arecibo observations allow us to resolve the HI absorption profile into its individual components. As the measured optical depths are much smaller than unity, this can be used to obtain information on the temperatures of the different phases of

neutral hydrogen in the absorber. Optically thin absorption lines have Gaussian shapes if the absorbing gas has a thermal distribution. The kinetic temperature  $T_k$  of the gas is then related to the velocity width of the absorption profile by

$$T_k = 21.87 \times \Delta V^2 \text{ K} , \quad (4)$$

where  $\Delta V$  is the FWHM of the Gaussian line in  $\text{km s}^{-1}$ . In fact, the measured velocity width provides an upper limit to the kinetic temperature, even in cases of non-thermal contributions to the line width, since the measured width must be *larger* than (or equal to) the width due to thermal motions. Thus, given sufficient velocity resolution, one can obtain the kinetic temperatures (or upper limits on  $T_k$ ) of the different absorption components, and then, using equation (3), their HI column densities (since  $T_s \approx T_k$ , see Kulkarni & Heiles 1988). This gives an independent estimate of the HI column density of the absorber, which can be compared to that obtained from the Lyman- $\alpha$  profile.

Since the narrow component seen in the Arecibo and GMRT spectra is asymmetric and there is additional broad weak absorption, we attempted to simultaneously fit three Gaussians to the absorption profile. The 3.125-MHz Arecibo spectrum was again used for this purpose. (Attempts were also made to fit only two Gaussians to the spectrum but, as expected, this was found to leave large residuals.) The three component fit to the 3.125-MHz spectrum decomposes the central feature into two components, the first with a velocity width (FWHM)  $\Delta V_1 = 3.76 \pm 0.12 \text{ km s}^{-1}$  and peak optical depth  $\tau_1 = 0.076 \pm 0.002$ , and the second with  $\Delta V_2 = 2.87 \pm 0.25 \text{ km s}^{-1}$  and  $\tau_2 = 0.022 \pm 0.004$ . The third, wide component has an FWHM of  $\Delta V_3 = 18.65 \pm 1.11 \text{ km s}^{-1}$  and a peak optical depth  $\tau_3 = 0.0046 \pm 0.0004$ . This best-fit model is superposed on the Arecibo 3.125-MHz spectrum in Figs. 1[C] and [D]; here, the fit is shown as a solid line, while the open squares indicate the original spectrum. Fig. 1[E] shows the spectrum after subtracting the two Gaussians fit to the narrow central component; the third, wide component is clearly visible. This spectrum also shows the fit to the wide component (solid line), which appears quite reasonable. Finally, Fig. 1[F] shows the spectrum after subtracting all three Gaussian components. The residuals are seen to lie within the noise.

The 0.781-MHz bandwidth Arecibo spectrum (shown in Fig. 2) has far lower sensitivity than the 3.125-MHz spectrum (owing to a much shorter integration time). It is consequently not very sensitive to the wide component. An independent check of the fit to the narrow components can however be made by fitting solely to these components, while keeping the parameters of the wide component fixed at the values determined from the 3.125-MHz spectrum. The parameters obtained from this fit agree (within the errors) with those listed above for the 3.125-MHz spectrum although there is a suggestion that the secondary narrow component may be even narrower than determined from

Component		1	2	3
Optical depth	AO Low	$0.076 \pm 0.002$	$0.022 \pm 0.004$	$0.0046 \pm 0.0005$
	GMRT			$0.0055 \pm 0.0005$
	AO High	$0.080 \pm 0.002$	$0.016 \pm 0.007$	
FWHM (km s $^{-1}$ )	AO Low	$3.76 \pm 0.12$	$2.87 \pm 0.25$	$18.65 \pm 1.11$
	GMRT			$18.77 \pm 1.82$
	AO High	$3.85 \pm 0.30$	$1.75 \pm 0.69$	
$T_k$ (K)		$308 \pm 24$	$180 \pm 30$	$7600 \pm 1250$
	$N_{\text{HI}}$ (10 $^{20}$ cm $^{-2}$ )	$1.7 \pm 0.24$	$0.21 \pm 0.1$	$12.6 \pm 4.9$
Redshift ( $\pm 10^{-6}$ )		0.221250	0.221240	0.221239

**Table 1.** Parameters of the multi-Gaussian fits to the different spectra. AO Low is the Arecibo 3.125-MHz bandwidth spectrum, GMRT is the GMRT 1.0-MHz bandwidth spectrum, and AO High is the Arecibo 0.78125-MHz bandwidth spectrum. The kinetic temperature,  $N_{\text{HI}}$  and redshift are computed from the AO Low spectrum, which has by far the best signal-to-noise ratio.

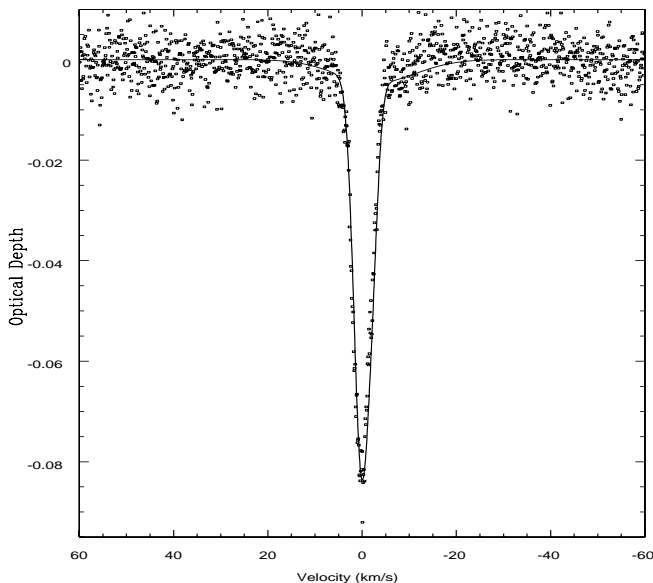


**Fig. 2.** High resolution ( $\sim 0.1$  km s $^{-1}$ ) Arecibo HI 21-cm spectrum of the  $z = 0.2212$  absorber towards OI 363 (open squares). The thin solid line is the fit derived from the  $\sim 0.4$ -km s $^{-1}$  Arecibo data.

the latter. Similarly, because of its relatively poor resolution, the GMRT spectrum is not particularly sensitive to the decomposition of the narrow component. However, the fit to the wide component (as obtained after keeping the parameters of the narrow components fixed to the values obtained from the 3.125-MHz Arecibo spectrum) is in ex-

cellent agreement with that obtained independently from the Arecibo data. Table 1 summarises the parameters of the fits to the different spectra.

Equation (4) can now be used to obtain the kinetic temperatures of the individual Gaussian components, using the velocity widths listed in Table 1. This yields  $T_{k_1} = 308 \pm 24$  K and  $T_{k_2} = 180 \pm 30$  K, for the two narrow components, and  $T_{k_3} = 7600 \pm 1250$  K, for the broad component. Clearly, the measured spin temperature  $T_s = 890 \pm 160$  K is quite different from the physical temperatures of the absorbing clouds. The kinetic temperatures of the first two components are larger than those of cold clouds in the Milky Way (Braun & Walterbos 1992), while the temperature of the third ( $T_k \sim 7600$  K) is in excellent agreement with estimates of the temperature of the WNM ( $\sim 5000 - 8000$  K; Kulkarni & Heiles 1988, Carilli et al. 1998). Note that recent Arecibo observations of the WNM in the Milky Way have found some evidence for *lower* temperatures than the above, with  $T_k \sim 2000$  K (Heiles & Troland 2000, Heiles 2001), although these results are still in preliminary form.

These estimates of the kinetic temperature can be used in equation (3) to obtain the HI column densities of the different components. This yields  $N_{\text{HI}}(1) = 1.7 \pm 0.24 \times 10^{20}$  cm $^{-2}$  and  $N_{\text{HI}}(2) = 2.1 \pm 1.0 \times 10^{19}$  cm $^{-2}$  for the two narrow components, and  $N_{\text{HI}}(3) = 1.26 \pm 0.49 \times 10^{21}$  cm $^{-2}$  for the wide component. The total column density in all three components is  $N_{\text{HI}} = 1.45 \pm 0.49$  cm $^{-2}$ , larger than (but, given the errors, still in agreement with) the value of  $7.9 \pm 1.4 \times 10^{20}$  cm $^{-2}$  obtained from the Lyman- $\alpha$  line (Rao & Turnshek 1998). Given that the 21-cm  $N_{\text{HI}}$  measurements are, strictly speaking, upper limits,

since there may be non-thermal contributions to the line width, the agreement between the column densities obtained from the 21-cm profile and the Lyman- $\alpha$  profile is quite good. Thus, the 21-cm profile of this absorber agrees fairly well with what would be expected from an absorber with a multi-phase medium much like that of the Galaxy (at least, in terms of the *temperatures* of the two phases).

It should be noted that non-thermal motions of a given magnitude will make a larger difference to narrow lines than to wide lines. It is therefore likely that the column density in the narrow components (which we identify with the CNM) are more severely over-estimated. The total contribution of the CNM to the HI column density is  $N_{\text{HI}}(\text{CNM}) \leq 1.9 \pm 0.25 \times 10^{20} \text{ cm}^{-2}$ , i.e. at most 24% of the total column density obtained from the damped Lyman- $\alpha$  line (Rao & Turnshek 1998). Of course, it is possible that the wide component also has a low kinetic temperature and that its large width is primarily due to non-thermal motions of the absorbing gas. For example, this could be due to the blending of a number of narrow CNM lines of low optical depth, rather than due to absorption by the WNM. Even in such a situation, however, the total contribution of such clouds to the HI column density would be very low, leaving unaccounted a substantial fraction of the column density, which must lie in a still hotter component. For example, if we assume that the hypothetical blended cold clouds have kinetic temperatures  $T_k \sim 100 \text{ K}$ , then the total HI column density in the wide component is negligible,  $N_{\text{HI}} \sim 1.7 \times 10^{19} \text{ cm}^{-2}$ . The bulk of the gas seen in the Lyman- $\alpha$  profile would hence still be required to be in a phase whose temperature is sufficiently large to make the 21-cm optical depth lower than our detection threshold. Thus, regardless of whether or not the wide component is identified with the WNM, one requires  $\sim 76\%$  (or possibly, even more) of the HI to be contained in the WNM. Indeed, the mere fact that we observe components in the absorption profile whose kinetic temperatures are smaller than the average spin temperature of the gas means that the gas must have multiple phases, including a warm phase. Given the relatively good agreement between the damped Lyman- $\alpha$  and 21-cm HI column densities and the reasonable value of the derived kinetic temperature of the wide component, we consider it highly likely that the wide component is indeed gas in the WNM phase. Note that in calculating the fraction of gas in the WNM phase we have assumed that the damped Lyman- $\alpha$   $N_{\text{HI}}$  measurement is the best estimate of the total neutral-hydrogen column density.

#### 4. Discussion

As discussed in the previous section, the 21-cm absorption profile of the  $z = 0.2212$  DLA is in excellent agreement with that expected were the absorption to arise in a multi-phase medium similar to that of the Milky Way. However, unlike the Galaxy, where the CNM and WNM both make equitable contributions to the total HI column density (Kulkarni & Heiles 1988),  $\sim 75\%$  of the neutral

hydrogen along this line of sight through the DLA must be in the warm phase, i.e. with temperature  $\sim 8000 \text{ K}$ , in order to account for its high estimated spin temperature.

The average spin temperature for the  $z = 0.2212$  absorber of  $\sim 900 \text{ K}$  is far higher than the typical spin temperatures of  $100 - 200 \text{ K}$  found in the Galaxy and nearby spirals (Braun & Walterbos 1992, Braun 1997). High spin temperatures of similar magnitude were earlier obtained by Carilli et al. (1996) in DLAs at high redshift. It was suggested there that the high  $T_s$  values at high  $z$  might be explained by evolutionary effects. Since then, however, there has been a substantial increase in the number of DLAs with 21-cm observations (Lane et al. 1998, Chengalur & Kanekar 1999, Chengalur & Kanekar 2000, Kanekar & Chengalur 2001) and, as Chengalur & Kanekar (2000) point out, high spin temperatures appear to be typical for DLAs at all redshifts. So far, the only DLAs which show low  $T_s$  values are those known to be associated with the disks of spiral galaxies. Chengalur & Kanekar (2000) (see also Kanekar & Chengalur 2001) suggested that the high- $T_s$  DLAs were likely to be associated with dwarf or LSB-type galaxies, where a combination of low central pressures, low dust content and low metallicities result in a smaller fraction for the CNM. Our conclusion that  $\sim 75\%$  of the gas along the line of sight through the  $z = 0.2212$  DLA is in the WNM phase is in good agreement with the observations of Young et al. (2000), who find that nearby dwarf galaxies have  $\sim 80\%$  of their neutral gas in the WNM phase.

Apart from possible selection effects, the association of DLAs with dwarf galaxies is somewhat surprising, both because of the existing paradigm of DLAs being associated with massive rotating disks (Prochaska & Wolfe 1997, Prochaska & Wolfe 1998), and the expectation (based on a census of the HI content of  $z = 0$  optically catalogued galaxies by Rao & Briggs 1993) that the bulk of the neutral HI at low redshifts is in large spiral galaxies. However, blind searches for HI emission at low redshift (i.e. unbiased by the presence of a catalogued galaxy; Schneider et al. 1998, Rosenberg & Schneider 2000) also indicate that there could be substantial amounts of HI in optically faint galaxies, although these results are still controversial (e.g. see Zwaan et al. (1997), for an opposing point of view).

In this context, it is of interest that the three lowest redshift DLAs known have all been (tentatively) identified as dwarf (or LSB) galaxies (Bowen et al. 2001, Turnshek et al. 2001, Cohen 2001) (where, following Turnshek et al. 2001, we only consider systems to be DLAs if they meet the “classical” selection criterion for a DLA, i.e. for which an observed Lyman- $\alpha$  profile yields an HI column density  $N_{\text{HI}} \geq 2 \times 10^{20} \text{ cm}^{-2}$ ). In the case of the current absorber, Le Brun et al. (1997) suggested that a galaxy at an impact parameter of  $\sim 6''$  from OI 363 was likely to be the DLA host. The spectrum of this galaxy (Cohen 2001) confirms that it is indeed at the correct redshift to produce the damped absorption. Turnshek et al. (2001) present both detailed multi-wavelength photome-

try and optical spectroscopy of this system, and find that its colours are consistent with a dwarf ( $L \sim 0.1L_*$ ) early-type galaxy. The radial profile, however, indicates the presence of both a bulge and a disk. Hence, these authors suggest that this galaxy could be the equivalent of the dwarf spirals seen at low redshifts (Schombert et al. 1995) and/or might have evolved from the faint blue galaxies seen at higher redshifts. It should also be noted that the impact parameter ( $\sim 18$ ) kpc is somewhat large for a dwarf galaxy and it is thus also possible that the absorption arises in an even fainter companion galaxy.

The present detection of the WNM in the  $z = 0.2212$  absorber towards OI 363 is the second case of evidence for a multi-phase medium in an extragalactic system. Lane et al. (2000) found that the  $z = 0.0912$  absorber towards the same quasar also has a multi-phase medium, with at most  $\sim$  one-third of the gas in the CNM phase. Interestingly, this DLA is also likely to be associated with a dwarf galaxy; Turnshek et al. (2001) place an upper limit of  $\sim 0.1 L_*$  on its K band luminosity. It is possible that such systems dominate current samples of DLAs because the obscuration for lines of sight passing through gas with both high metallicity and high dust content might well be sufficient to make medium resolution spectroscopy of the background quasar extremely difficult (Fall & Pei 1993).

As conjectured earlier, the high observed spin temperatures of DLAs thus seem to be a consequence of their having a higher fraction of the WNM than is found for the Galaxy. The fact that the two lowest redshift known DLAs have high  $T_s$  means that this cannot be due to evolutionary effects. The possibility that it is due to a selection effect (i.e. a bias against highly obscured lines of sight) cannot, however, be ruled out. Such a bias can only be properly quantified by searches for DLAs against bright radio sources, regardless of their optical magnitude. Several such searches are currently under way (see e.g. Ellison 2000) and an observational determination of the importance of dust obscuration should be available in the near future.

**Acknowledgements.** We are grateful to Phil Perillat and Chris Salter for their help with observations and data reduction and to Chris for detailed comments and suggestions on an earlier draft of this paper. We also thank Frank Briggs for illuminating discussions on the “double-switched” mode of observation. The NAIC is operated by Cornell University under a cooperative agreement with the NSF. The GMRT observations presented in this paper would not have been possible without the many years of dedicated effort put in by the GMRT staff to build the telescope.

## References

Bowen D. V., Tripp T. M., Jenkins E. B., 2001, AJ, 121, 1456.  
 Braun R., Walterbos R., 1992, ApJ, 386, 120.  
 Braun R., 1997, ApJ, 484, 637.  
 Carilli C. L., Lane W., de Bruyn A. G., Braun R., Miley G. K., 1996, AJ, 111, 1830.  
 Carilli C. L., Dwarakanath K. D., Goss W. M., 1998, ApJ, 502, L79.  
 Cohen J. G., 2001, AJ, 121, 1275.  
 Chengalur J. N., Kanekar N., 1999, MNRAS, 302, L29.  
 Chengalur J. N., Kanekar N., 2000, MNRAS, 318, 303.  
 Ellison S. L., 2000, Ph. D. Thesis, Cambridge Univ.  
 Fall S. M., Pei Y. C., 1993, ApJ, 402, 479.  
 Haehnelt M. G., Steinmetz M., Rauch M., 1998, ApJ, 495, 64.  
 Heiles C., Troland T., 2000, NAIC Newsletter 30, 9.  
 Heiles C., 2001, in The Fourth Tetons Summer Conference: Galactic Structure, Stars and the Interstellar Medium, eds. M. D. Bicay and C. E. Woodward (astro-ph:0010047).  
 Kanekar N., Chengalur J. N., 2001, A&A, 369, 42.  
 Kulkarni S. R., Heiles C., 1988, in Galactic and Extra-Galactic Radio Astronomy (2nd edition), G. Verschuur & K. I. Kellermann eds., Springer-Verlag (Berlin and New York), 95.  
 Lane W., Smette A., Briggs F. H., Rao S. M., Turnshek D. A., Meylan G., 1998, AJ, 116, 26.  
 Lane W., Briggs F. H., Smette A., 2000, ApJ, 532, 146.  
 Lanzetta K. M. & Bowen D. V., 1992, ApJ, 391, 48.  
 Le Brun V., Bergeron J., Boissé P., Deharveng J.-M., 1997, A&A, 321, 733.  
 Ledoux C., Petitjean P., Bergeron J., Wampler E. J., Srianand R., 1998, A&A, 337, 51.  
 McDonald P., Miralda-Escude J., 1999, ApJ, 519, 486.  
 Prochaska J. X., Wolfe A. M., 1997, ApJ, 487, 73.  
 Prochaska J. X., Wolfe A. M., 1998, ApJ, 507, 113.  
 Rao S. M., Briggs F. H., 1993, ApJ, 419, 515.  
 Rao S. M., Turnshek, D. A., 1998, ApJ, 500, L115.  
 Rosenberg J. L., Schneider S. E., 2000, ApJS, 130, 177.  
 Schneider S. E., Spitzak J. G., Rosenberg J. L., 1998, ApJ 507, L9.  
 Schombert J. M., Pildis R. A., Eder J. A., Oemler A., 1995, AJ, 110, 2067.  
 Stanghellini C., Dallacasa D., O’ Dea C. P., Baum S. A., Fanti R., Fanti C., 1997, A&A, 325, 943.  
 Storrie-Lombardi L., Wolfe A. M., 2000, ApJ, 543, 552.  
 Turnshek D. A., Rao S. M., Lane W., Monier E., Nestor D., 2000, to appear in proceedings of the “Gas and Galaxy Evolution” conference, J. E. Hibbard, M. P. Rupen and J. H. van Gorkom eds. (astro-ph:0009096).  
 Turnshek D. A., Rao S. M., Nestor D., Lane W., Monier E., Bergeron J., Smette A., 2001, submitted to ApJ (astro-ph/0010573).  
 Wolfe A. M., 1988, in QSO Absorption Lines: Probing the Universe, J. C. Blades et al. eds., Cambridge University Press.  
 Wolfire M. G., Hollenbach D., McKee C. F., Tielens A. G. G. M., Bakes E. L. O., 1995, ApJ, 443, 152.  
 Young L. M., van Zee L., Dohm-Palmer R. C., Lo K. Y., 2000, to appear in proceedings of the conference “Gas and Galaxy Evolution”, J. E. Hibbard, M. P. Rupen and J. H. van Gorkom eds., (astro-ph:0009069).  
 Zwaan M. A., Briggs F. H., Sprayberry D., Sorar E., 1997, ApJ 490, 173.

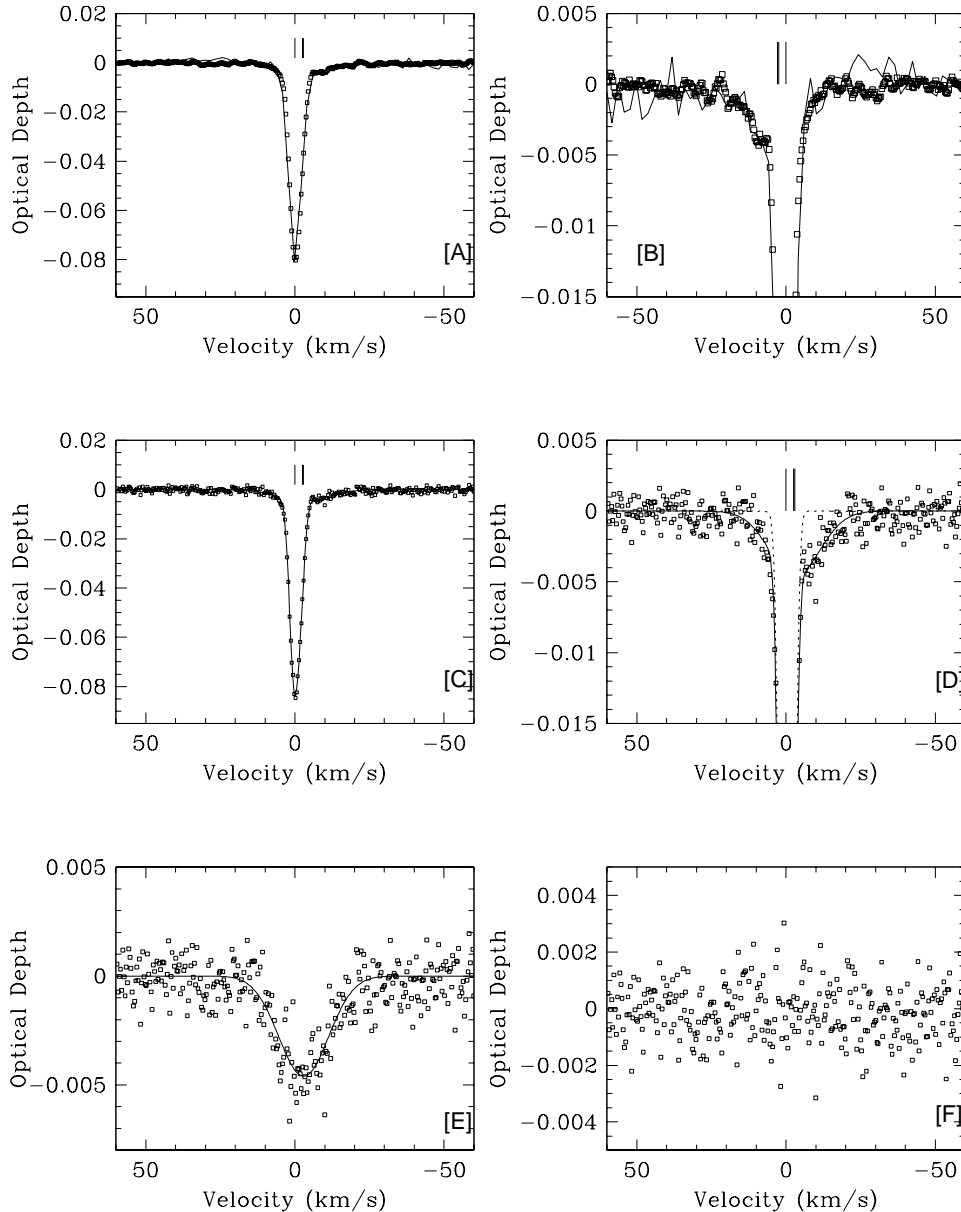


**Fig. 1.** The 21-cm absorption spectra of the  $z = 0.2212$  absorber towards OI 363. [A] A comparison of the Arecibo  $0.4\text{-km s}^{-1}$  resolution spectrum (open squares) with the GMRT  $2.0\text{-km s}^{-1}$  resolution spectrum (shown as a thin solid line). The Arecibo spectrum has been smoothed to a resolution of  $\sim 2\text{ km s}^{-1}$  for the comparison. **The vertical lines above  $\tau = 0$ , indicate the locations of the centres of the three components.** [B] The  $0.4\text{-km s}^{-1}$  resolution Arecibo spectrum (open squares) shown superposed with the GMRT  $2.0\text{-km s}^{-1}$  resolution spectrum (solid line). This is a zoomed-in version of panel [A] to bring out the shallow absorption wing seen in both spectra. The Arecibo spectrum has again been smoothed to a resolution of  $\sim 2\text{ km s}^{-1}$  for the comparison. [C] The  $0.4\text{-km s}^{-1}$  resolution Arecibo spectrum (open squares) with the three-component Gaussian fit shown as a thin solid line. (see the text and Table 1 for the fit parameters). [D] The  $0.4\text{-km s}^{-1}$  resolution Arecibo spectrum (open squares) shown superposed with the multi-Gaussian fit (thin solid line). This is a zoomed-in version of panel [C] to bring out the shallow absorption wing. **The dotted line is a two-component Gaussian fit, which clearly brings out the necessity of including a wide component.** [E] Residuals left after subtracting the two narrow components from the  $0.4\text{-km s}^{-1}$  resolution Arecibo spectrum (open squares). The fit to the wide component (see text and Table 1) is shown as a thin solid line. [F] Residuals left after subtracting the two narrow components and the wide component from the  $0.4\text{-km s}^{-1}$  resolution Arecibo spectrum.